Wavelength Blocking Filter With Flexible Data Rates and Channel Spacing

Roland Ryf, *Member, IEEE*, Yikai Su, *Member, IEEE*, Lothar Möller, *Member, IEEE*, S. Chandrasekhar, *Fellow, IEEE*, Xiang Liu, *Member, IEEE*, David T. Neilson, *Senior Member, IEEE, Member, OSA*, and C. Randy Giles, *Fellow, OSA*

***Abstract*—This paper presents a high-resolution (13.2 GHz) channel-blocking optical filter, suitable for use as a reconfigurable optical add/drop multiplexer (ROADM), which seamlessly supports data rates from 2.5 to 160 Gb/s. The filter consists of a linear array of 64 MEMS micromirrors and a high-dispersion echelle grating. The demonstrated device had an insertion loss of 9 dB, a loss ripple of 1.2 dB, and a group delay ripple of 15 ps. Data transmission through the device with various mixed data rate scenarios ranging from 2.5 to 160 Gb/s showed negligible penalty, except at 40 Gb/s where a maximum penalty of 1.5 dB was observed due to a phase coherence with the blocker filter ripple.**

***Index Terms*—Gratings, microelectromechanical devices, optical filter, optical switches.**

I. Introduction

MANAGEMENT of wavelength channels directly in the optical domain is rapidly gaining importance with the increasing transparency of optical transport systems. However, the current generation of wavelength-managing reconfigurable optical add/drop multiplexers (ROADMs) are designed for specific channel locations and data rates [1]–[6], thereby necessitating complete OADM replacement when upgrading line systems to higher channel densities or higher-rate channels. In this paper, we present an optical blocking filter having a frequency resolution of 13.2 GHz (much narrower than typical channel spacings of 50 or 100 GHz), that can be used to build ROADMs capable of seamlessly adapting to most channel plans and line system upgrades. Multiple contiguous 13.2 GHz slots can be combined to form wider passbands, allowing programming of both the width and the location of the selected wavelength-division multiplexed (WDM) channels. The principle is schematically shown in Fig. 1 and was to our knowledge only shown previously as a combination of two 50-GHz spaced channels [7] to support 40 Gb/s signals. The filter described in this paper exhibits a three-times-higher spectral resolution, enabling greatly increased channel plan flexibility. It is based on a free space diffraction grating combined with a linear array of single tilt axis microelectromechanical-system (MEMS) micromirrors. The device can be extended into an add/drop multiplexer introducing additional optical elements as described in [3] or by using a broadcast and select architecture [8]–[11].

Manuscript received June 21, 2004; revised October 4, 2004.

R. Ryf, L. Möller, S. Chandrasekhar, X. Liu, D. T. Neilson, and C. R. Giles are with Bell Laboratories, Lucent Technologies, Holmdel, NJ 07733 USA (e-mail: ryf@lucent.com).

Y. Su was with Bell Laboratories, Lucent Technologies, NJ 07733 USA. He is now with the State Key Lab of Advanced Optical Communication Systems and Networks, Shanghai Jiao Tong University, Shanghai 200030, China (e-mail: yikaisu@sjtu.edu.cn).

Digital Object Identifier 10.1109/JLT.2004.840346

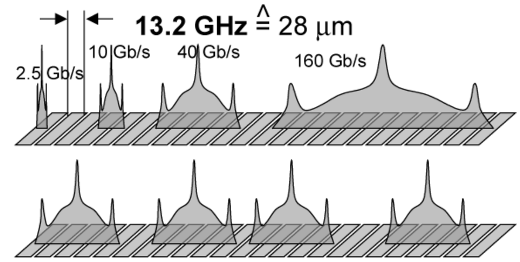

Fig. 1. Principle of high resolution blocking filter. (a) Support for different data rates. (b) Nonuniformly spaced channels.

In the present paper, the device was operated in three different regimes: first with a data rate of 2.5 Gb/s which has a spectral width that is narrower than the channel slots; second with a data rate of 10 Gb/s whose spectrum is covered by two slots; third with 40 Gb/s nonreturn-to-zero (NRZ) and 160 Gb/s carrier suppressed return-to-zero (CSRZ) signals where 8 to 32 slots were used to cover the required spectral widths. All three configurations stress the optical performance of the device in different ways. For data rates smaller than the channel slot spacing, the passband in the slot must be flat and wide, whereas in the situation when the modulated signal covers multiple slots, the loss ripple appearing at the slot boundaries will impact the optical performance.

The largest penalty was observed when detuning the central wavelength of a 40 Gb/s signal. We present a numerical analysis confirming that the loss ripple in the passband is the origin of the penalty, and how the penalty is impacted by the spectral width of the slot.

We also report transmission and crosstalk measurements performed at mixed 2.5, 10, 40, and 160 Gb/s CSRZ signals, confirming the viability of the proposed device.

II. High-Resolution Wavelength Blocking Filter

The optical design of the filter [12]–[14] is shown in Fig. 2. The light is brought into the filter by a fiber, which after an optical circulator, is launched into free space, then collimated by a multielement lens. The collimated light reaches an echelle grating where it is angularly dispersed as function of the wavelength. The grating, arranged near Littrow geometry, had 52.67 lines/mm and operated in the twenty-second order with low polarization dependent loss (PDL) (<1 dB) over the entire C-band. After a second pass through the lens, the wavelength-separated

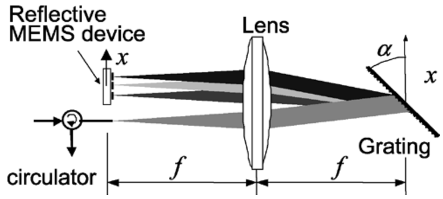

Fig. 2. Schematic optical design of the blocking filter.

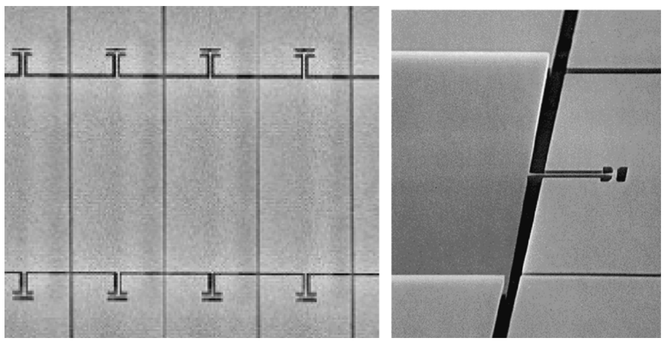

Fig. 3. Picture of single-crystal torsion silicon micromechanical tilt mirror array with a device pitch of 29 μm and tilt angle is up to 8 degrees.

beams were focused on the MEMS micromirrors. In the case where the micromirrors were perpendicular to the incident beam, the beam retraced the same path and coupled into the fiber where the output is separated by the optical circulator. Tilting mirrors result in the beam reaching the fiber under an angle and therefore introduce an angle-dependent loss. The input and output of the system are self-aligning as a single lens is used to collimate the light from the fiber onto the grating and to focus the spectrally widened spots on the MEMS device. Also the double pass on the gratings guarantees a minimal group delay variation among the wavelength channel slots.

The MEMS device was a linear array of 64 micromirrors, having a tilt axis orthogonal to the array direction and having a spacing of 27.2 to 29.6 μm to match the nonlinear dispersion of a previous lower resolution blocker system [12], [13]. A single crystal silicon fabrication process [17] was used to make the torsion mirror array shown in Fig. 3 and the device is aluminum coated to give high reflectivity at 1.55 μm. Torsion rods are used as springs and the mirrors have a tilt range of $\pm 8^\circ$. The mirrors are actuated using electrostatic force from electrodes on an electrode chip placed below the mirror chip. Maximal actuation voltage was 120 V. The mirror chips were fabricated using 1-μm-thick SOI which resulted in fast devices with resonant frequencies exceeding 20 kHz. To obtain a reproducible gap between the two chips, accurate hard stops were built using silicon oxide posts on the electrode chip. To guarantee a high filling factor along the dispersion direction, a 248-nm SUV stepper is used to define submicrometer wide springs and very small lateral gaps between the mirrors (0.4 μm). The mirrors had a tilt range of 0–8°, and were actuated electrostatically with a maximal activation voltage of 120 V. The nominal 28 μm width of the mirrors in the array direction and 50 μm in the orthogonal direction, are much larger than the 10 μm spot size of the light beam. The ratio between spot-size and mirror width is responsible for the passband shape [13], and in our case a flat and wide passband was expected. The channel spacing of the filter was determined by the dispersion of the grating and the focal length f of the collimating lens. The collimating lens was a multielement lens with a focal length of 100 mm [3]. For a grating mount angle $\alpha = 63.5^\circ$ the spatial dispersion $\Delta x/\Delta\lambda$ of the filter is given by

$$\frac{\Delta x}{\Delta\lambda} = \frac{2f}{\lambda_0}\tan(\alpha) \quad (1)$$

where λ_0 is the central wavelength of the filter. For our geometry, the micromirror spacing of 29 μm corresponded to a spectral separation of 116 pm or 13.2 GHz.

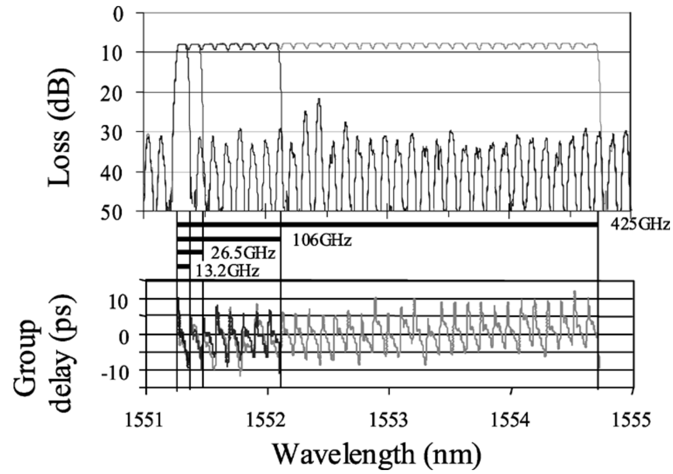

Fig. 4. Transmission and group delay for a channel width of 13.2, 26.5, 106, and 425 GHz.

The optical transmission and group delay for single and multiple mirrors in the on-state are shown in Fig. 4. The insertion loss for the mirrors in the nominally undeflected state was 9 dB. The sources of the loss were: 2.5 dB for the double pass diffraction efficiency of the grating, 1.5 dB from the circulator, 0.3 dB from the reflectivity of the MEMS device, and 4.7 dB attributed to loss from the antireflection coatings of the five element lens, and to mode mismatch on four passes through the lens. The loss ripple between adjacent channels was <1.5 dB and resulted from the presence of a gap and a phase discontinuity between the mirrors. The PDL of the device primarily resulted from the grating diffraction is <1.1 dB.

The group delay for undeflected mirrors shows a small overall chromatic dispersion of 1 ps/nm, and some ripples with 15 ps peak-to-peak value, accentuated at the gaps of the mirrors. The ripples can be explained by the presence of a small a phase jump originating from the mirrors not having the same position in the out-of-plane direction. This happens in the case where the mirror exhibits a small tilt angle variation in the nominally untilted condition. Group delay ripple is also produced by discontinuity of the spatial phase derivative in the array direction. This can occur for example if the mirrors are not flat. For perfectly flat mirrors, a constant group delay is expected inside the passband of the micromirrors. For our switch, we observe an approx-

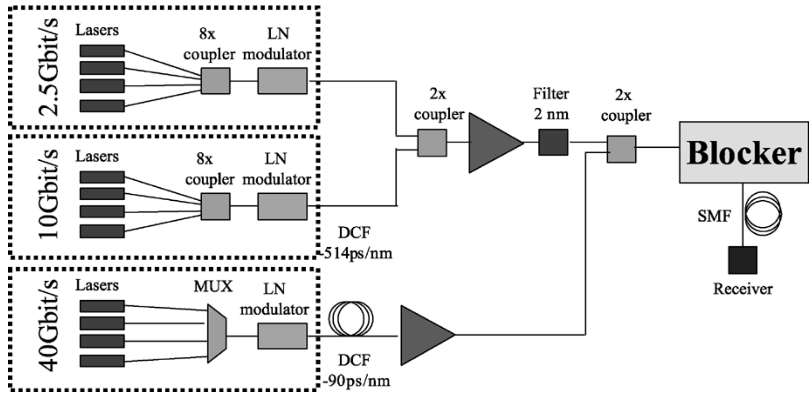

Fig. 5. Setup for testing the blocking filter on a WDM signal with different rates and channel spacings.

imately linear group delay change of $\Delta\tau_g/\Delta\lambda = 87.5\ \mathrm{ps/nm}$, which indicates that the mirrors have a radius of curvature of

$$R_c = \frac{4f^2\tan^2(\alpha)}{\frac{c\lambda_0\Delta\tau_g}{\Delta\lambda}} = 4\ \mathrm{mm} \tag{2}$$

which is not optimal for the performance of the switch [15]. The micromirror exhibited such a strong curvature, because this particular mirror array was used for optomechanical housing alignment testing and has undergone several high temperature cycles ($> 400\,^\circ\mathrm{C}$). Typical curvature of the micromirrors before the high temperature cycling, is in the order of several tens of millimeters, and therefore with negligible effect on the optical performance.

Applying Fourier theory for linear systems, it can be shown that any periodic perturbation of either the transmission or the phase of a filter, will lead to generation of signal copies in the time domain which are delayed with respect to the main signal by multiple of the time constant [16]

$$\tau_p = \frac{1}{\Delta\omega} = 76\ \mathrm{ps}. \tag{3}$$

Here $\Delta\omega = 13.2$ GHz is the period of perturbation in the frequency space. The amplitude of the signal copy will depend on the extent of the perturbation, and for the measured transmission and group delay of our filter a rejection of a signal copy of more than 30 dB is expected. For such a rejection, negligible penalty is expected as long τ_p is not a close multiple of the bit period of the data signal. We expected a penalty at a data rate of 40 Gb/s (bit period of 25 ps), resulting from our filter creating a signal copy having a three bit-delay. This coincidence can be avoided by changing the mirror width according to (1) and for example by setting the channel spacing to 12.5 GHz, which also would lead to a spacing compatible with the ITU standards.

The differential group delay (DGD) also shows a periodic behavior similar to the group delay and is typically <1 ps across a channel and exhibits maximum excursions of <5 ps. The origin of the DGD is likely polarization dependent scattering at the edges of the micromirrors.

In the blocking state mirrors are deflected at their maximum tilt angle, as limited by a mechanical stop. In this state the mean loss over a channel is 38 dB with peaks as high as 24 dB, and a strong loss ripple. The origin of the ripples in this case are the phase jumps between neighboring mirrors. For micromirrors with tilt axes orthogonal to the array direction it is possible to operate the mirrors with multiples $\lambda/2$ of phase-matched jumps, for a discrete number of angles (four in current micromirror geometry). A homogeneous transmission in the blocked state is expected for mirrors tilting parallel to the array direction, where the phase matching is always obtained when the mirrors are tilted by the same angle [14], [17], [21].

In the transmission-state a periodic distortion is desirable in order to avoid pulse widening in the temporal domain; in the blocking configuration fast and aperiodic phase jumps are desirable to temporally spread the parasitic transmitted light. These aperiodic phase jumps in the blocking-state can be achieved by detuning the mirrors randomly over the range of $+/-1.5^\circ$.

The nonperfect blocking performance of our device resulted in crosstalk, which on average was < -29 dB with peaks at -15 dB located near the mirror boundary. The impact of the crosstalk is addressed in detail in the following section.

The device can also by extended in total wavelength range by adding more micromirrors on the MEMS device. The lens and grating in our prototype are capable of supporting the entire C-band, requiring an array of 320 mirrors. A larger array does not represent more difficult fabrication, but rather requires a package larger than that which was available and with a greater number of electrical interconnects.

III. Measurements With Multirate WDM Channels

To test the performance of the filter in a mixed channel spacing plan, the following signals were combined to create a multirate WDM signal: four 2.5 Gb/s NRZ at 13.2 GHz spacing, four 10 Gb/s NRZ at 27.5 GHz spacing, and four 40 Gb/s at 106 GHz channels spacing. The setup for the signal generation is shown in Fig. 5, and consists of three sections each carrying pseudorandom bit sequence (PRBS) $2^{31}-1$ data streams. The four 2.5 Gb/s and four 10 Gb/s signals, were optically multiplexed using a passive power combiner as no appropriate WDM multiplexer was available. The four 40 Gb/s signals were combined using a flat passband multiplexer having a nominal 100-GHz spacing. The channels were decorrelated using a dispersion-compensating fiber with -514 ps/nm dispersion for the 10 Gb/s signals and a standard single mode fiber with 90 ps/nm for the 40 Gb/s signals. The 2.5 Gb/s signals were not decorrelated by optical means, instead the neighboring

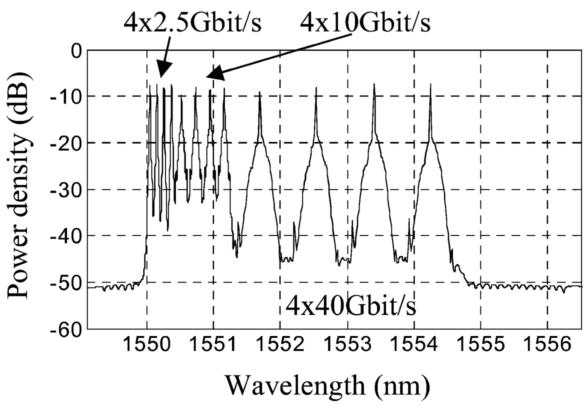

Fig. 6. Input spectrum of the WDM signal with different data rate and channel spacing.

TABLE I
TRANSMISSION PENALTY FOR DIFFERENT DATA RATES

Data rate (Gb/s)	Channel Spacing (GHz)	Trans. penalty (dB)	X-talk penalty (dB)	Tuning range[1] (GHz)
2.5	13.2	0	0.2	±5
10	26.5	0	0	±10
40	106	1.5	0	±25
160	425	0.2	n/a	n/a

[1]Detuning ranges are measured at 0.5dB penalty

channels were modulated by independent pattern generators for the crosstalk measurements.

The signals were then amplified, combined, and sent through the blocker, which was set to select one particular channel for detection. The 2.5 and 10 Gb/s signals were detected using an 8-GHz p-i-n detector, whereas the 40-Gb/s signals were detected with an optically preamplified receiver having a 32-GHz bandwidth. The spectra of the generated multirate signals are shown in Fig. 6 after traversing the blocking filter with all mirrors set in the on-state. In a separate experiment, the switch was tested using 160 Gb/s CSRZ signal [22] and a filter width of 425 GHz. The transmission penalties, out-of-band crosstalk penalties, and detuning ranges for the 2.5 to 160 Gb/s signals are listed in Table I and are discussed next.

A. Performance of a Single Mirror at 2.5 Gb/s

In this measurement, the central wavelength of the NRZ signal was centered in the middle of a micromirror, and the operation of the device is equivalent to that in previously reported MEMS-Blocker devices [12]–[14], with a three-times scaled-down spectrum and four-times reduced data rate. The transmission of the filter in this configuration is shown in Fig. 7(a) and exhibits a flat region in the center with a 3-dB bandwidth of 11.2 GHz. The penalty as a function of the misalignment between the data carrier and the filter is shown in Fig. 7(b). A large detuning range of ±5 GHz at a penalty of 0.5 dB can be seen. The penalty was measured for all 4×2.5 GHz channels spaced by 13.2 GHz, and appreciable penalty could be measured, whereas the worst-case crosstalk penalty was found to be 0.2 dB.

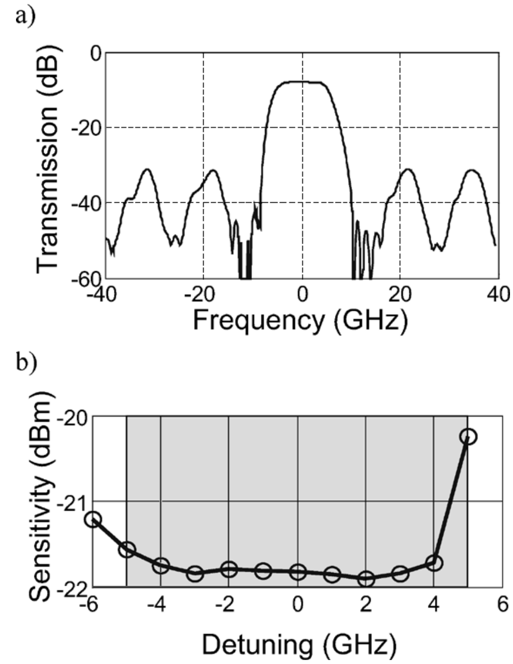

Fig. 7. (a) Transmission spectrum with a single mirror on. (b) Penalty for carrier detuning of a 2.5 Gb/s NRZ signal.

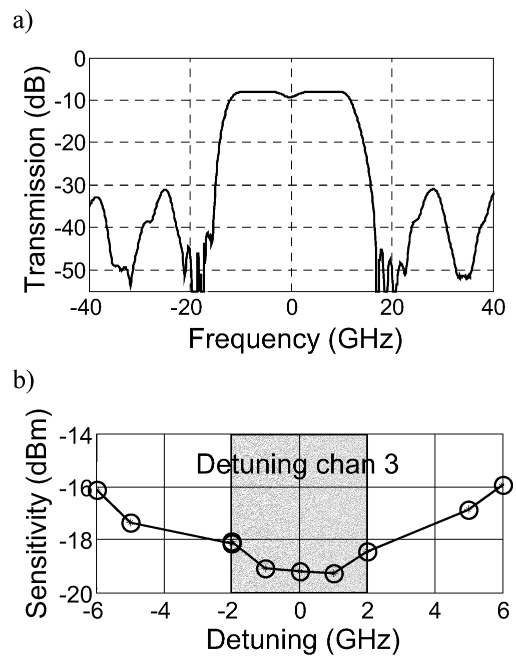

Fig. 8. (a) Transmission spectrum with two mirrors on. (b) Penalty for carrier detuning of a 10 Gb/s NRZ signal.

B. Performance of a Mirror Pair at 10 Gb/s

In this configuration, the carrier of a NRZ 10 Gb/s signal was centered between two adjacent mirrors, and the carrier peak experienced 1.5 dB attenuation [see Fig. 8(a)]. The 3-dB passband of the filter is 24.6 GHz, which is comparable to the spectral with of the 10 Gb/s NRZ signal. Note that the bandwidth of the filter was increased by a factor of two compared to the previous configuration but the data rate was scaled up by a factor of four, therefore representing twice the spectral efficiency.

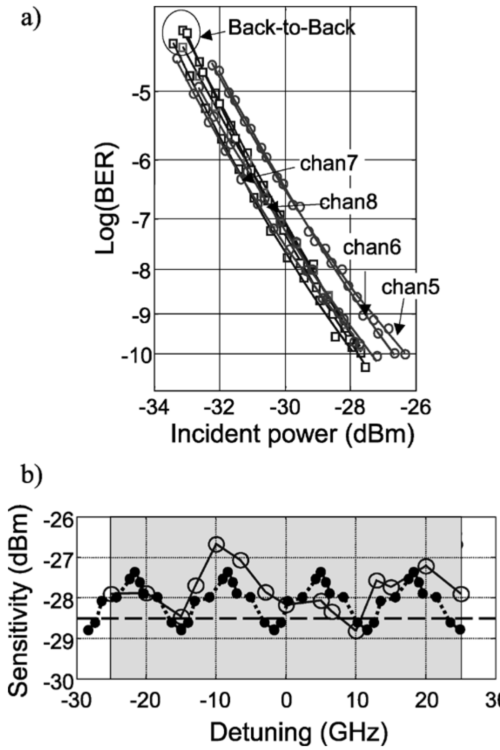

Fig. 9. (a) Bit error rate curves for a 40 Gb/s NRZ signal transmitted through the filter with 8 mirrors on. (b) Penalty for carrier detuning where the circle denote measured points and the dots are from a simulation.

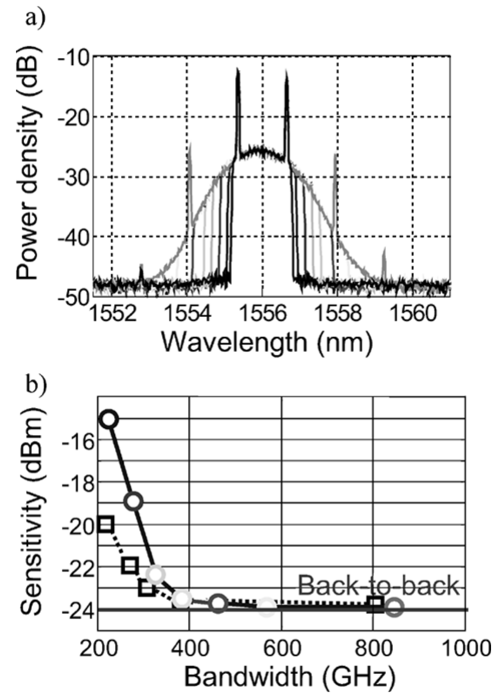

Fig. 10. Spectra of 160 Gb/s CSRZ signal filtered at different bandwidths. (a) Spectra of the filter signals. (b) Measured sensitivities are plotted as function of the filter width. Sensitivity as function of the bandwidth where the circle denote measurements and the square are from simulations.

For this configuration only negligibly small penalty or negative penalty of as much as -0.5 dB were observed for all of the four channels, and a limited tuning range of ± 2 GHz at <0.5 dB penalty was possible.

C. Performance of Eight Contiguous Mirror Segments at 40 Gb/s

The experiment was repeated using eight contiguous mirrors with a 40 Gb/s NRZ signal. As previously mentioned, the periodicity of the filter created a signal copy delayed by 76 ps, and thus impacted the signal quality of the transmitted signal. In particular, by detuning the filter, the phase of the signal copy can be modified, thus causing a variable amount of penalty. The measurements are shown in Fig. 9(b) where the measured penalties are represented by circles, and the dotted line is derived from numerical eye simulations [16], [23]. The measured penalties vary from -0.5 to 1.5 dB, whereas the simulation predicts a negative penalty of -0.2 dB for the centered filter and a maximal penalty of 1.4 dB at 6.7 GHz frequency offset. We note also that by eliminating the penalty caused by the filter periodicity, the tuning range was very wide (± 25 GHz) with no additional penalty. Furthermore, no crosstalk from neighboring channels was observed.

D. Performance of a Multimirror Segment at 160 Gb/s

The filter was also tested with a 160-Gb/s CSRZ signal. This measurement represents a very stringent test of group delay and differential group delay, because any delay comparable to the 3-ps pulsewidth will produce pulse broadening. A small penalty of ~ 0.2 dB was observed with the 160-Gb/s CSRZ signal and the 425-GHz filter bandwidth. The results are shown in Fig. 10. Our results at 160 Gb/s were also confirmed by numerical simulations depicted as dots in Fig. 10(b), predicting a 0.2-dB penalty for a filter width of 425 GHz.

As in the case of 40 Gb/s, we expected a signal copy to appear after 76 ps with a 12-bit delay. However, its effect appears to be very weak, possibly due to the significant pulse widening of the RZ 160 Gb/s signal copy.

E. Coherent Crosstalk Over Cascaded Blockers

In the previous section, the blocking filter was characterized for transmission penalty and crosstalk from adjacent channel at mixed data rates and channels spacing. This corresponds to the situation where the blocker is used to select a particular channel from the spectrum. In a transmission system, however, the blocker can also be used to block a particular channel, so that a new channel at the same wavelength can be added after the blocking filter, using for example a power combiner [9]–[13]. Any part of the channel that is not completely blocked by the device can therefore interfere with the new channel. To assess the system penalty due to this coherent crosstalk, we performed numerical simulations using the measured loss profile and group-delay profile of the blocker configured to provide an 850-GHz blocking band. The transmitter and receiver are assumed to be ideal. The signal in the temporal domain is Fourier transformed to the frequency domain, then the loss and group delay ripples are applied, and finally inverse Fourier transformed back to time domain. The optical signal-to-noise (OSNR) penalty is estimated through closure of the signal-amplitude eye, as discussed in [16], [23]. The simulated signal has a bit length of 128 bits, sufficient for the short-range penalties due to group-delay

TABLE II
COHERENT CROSSTALK PENALTY FOR DIFFERENT DATA FORMATS

Data rate (Gb/s)	Penalty 1 pass (dB)	Penalty 2 pass (dB)	Penalty 3 pass (dB)
10Gb/s NRZ	0.8	1.6	3
10Gb/s RZ	0.6	1.4	2.5
40Gb/s NRZ	0.5	1	2

and loss ripples [16]. For simplicity and easy comparison, we assumed the worst-case coherent crosstalk case, in which the signal is interfering with the noise having the same polarization, phase, and timing. The coherent crosstalk penalty calculated for 10 Gb/s NRZ and RZ and 40 Gb/s NRZ signals are shown in Table II for a single pass and cascaded transmission through a blocked bandwidth section of 185 GHz.

The highest single-pass penalty of 0.8 dB occurred for the 10 Gb/s NRZ signal, whereas the RZ signal is more tolerant. For 40 Gb/s NRZ, the penalty is further reduced to 0.5 dB. The origin of the penalty are the spectrally sharp transmission peaks present inside the blocked channel, therefore the penalty will vary strongly by detuning the central frequency of the filter in respect to the carrier frequency of the signal.

The worst-case penalty listed in Table II, coincided with the situation where the carrier wavelength is centered between the micromirrors. This situation might be avoided by detuning the filter, if allowed in the channel allocation map. Table II also shows how the penalty increases for cascaded blocked channels. A considerable penalty of 2–3 dB is found after three blocking stages, and mitigation of this impairment will require micromirrors with an orthogonal tilt axis as described in Section II.

IV. CONCLUSION

We have demonstrated a new wavelength blocker capable of subdata-channel-rate resolution. The blocker can be used as the central switching element of an OADM supporting variable bandwidths and channel locations. The transmission and out-of-band crosstalk were characterized for a multirate WDM signal subject to a blocking filter having a 13.2-GHz spectral resolution. The device caused negligible penalties for most data rates from 2.5 to 160 Gb/s, and a penalty of <1.5 dB for 40 Gb/s NRZ signals. Simulations of coherent crosstalk showed <1 dB penalty with lower penalty expected from improved micromirror design.

REFERENCES

[1] J. E. Ford, V. A. Aksyuk, D. J. Bishop, and J. A. Walker, “Wavelength add-drop switching using tilting micro-mirrors,” *J. Lightw. Technol.*, vol. 17, pp. 904–911, May 1999.

[2] J. Ford, “Micromechanical wavelength add/drop switching: from device to network architecture,” in *Proc. Optical Fiber Communication Conf. Exhibit*, 2003.

[3] D. M. Marom, D. T. Neilson, D. S. Greywall, N. R. Basavanhally, P. R. Kolodner, Y. L. Low, C. A. Bolle, S. Chandrasekhar, L. Buhl, S.-H. Oh, C. S. Pai, K. Werder, H. T. Soh, G. R. Bogart, E. Ferry, F. P. Klemens, K. Teffeau, J. F. Miner, S. Rogers, J. E. Bower, R. C. Keller, and W. Mansfield, “Wavelength selective 1 × 4 switch for 128 WDM channels at 50 GHz spacing,” in *Proc. Optical Fiber Communication Conf. Exhibit*, 2002, pp. 857–859.

[4] C. R. Doerr, L. W. Stulz, M. Cappuzzo, L. Gomez, A. Paunsecu, E. Laskowski, S. Chandrasekhar, and L. Buhl, “2 × 2 wavelength- selective cross connect capable of switching 128 channels in sets of eight,” *IEEE Photon. Technol. Lett.*, vol. 14, pp. 387–389, Mar. 2002.

[5] T. Ducellier, J. Bismuth, S. F. Roux, A. Gillet, C. Merchant, M. Miller, M. Mala, Y. Ma, L. Tay, J. Sibille, M. Alavanja, A. Deren, M. Cugalj, D. Ivancevic, V. Dhuler, E. Hill, A. Cowen, B. Shen, and R. Wood, “The MWS 1 × 4: a high performance wavelength switching building block,” in *Europ. Conf. Optical Communication*, vol. 1, Copenhagen, Denmark, Sept. 8–12, 2002, Paper: 2.3.1.

[6] M. C. Wu, J. C. Tsai, S. Huang, and H. Dooyoung, “MEMS WDM routers using analog micro-mirror arrays,” in *Proc. 15th Ann. Meet. IEEE LEOS*, vol. 2, Nov. 10–14, 2002, pp. 582–583.

[7] J. K. Rhee, F. Garcia, A. Ellis, B. Hallock, T. Kennedy, T. Lackey, R. G. Lindquist, J. P. Kondis, B. A. Scott, J. M. Harris, D. Wolf, and M. Dugan, “Variable passband optical add-drop multiplexer using wavelength selective switch,” in *Proc. 27th Europ. Conf. Optical Communication*, vol. 4, 2001, pp. 550–551.

[8] Y. Su, S. Chandrasekhar, R. Ryf, C. R. Doerr, L. Möller, I. Widjaja, G. Raybon, D. T. Neilson, T. Zhou, L. Buhl, and S. Radic, “A multi-rate upgradeable 1.6-Tb/s Hierarchical OADM network,” *IEEE Photon. Technol. Lett.*, vol. 16, pp. 317–319, Jan. 2004.

[9] M. Vasilyev, I. Tomkos, J. Rhee, M. Mehendale, B. Hallock, B. Szalabofka, M. Willams, S. Tsuda, and M. Sharma, “Broadcast and select OADM in 80 × 10.7 Gb/s ultra-longhaul network,” *IEEE Photon. Technol. Lett.*, vol. 15, pp. 332–334, Feb. 2003.

[10] M. Vasilyev, I. Tomkos, M. Mehendale, J.-K. Rhee, A. Kobyakov, M. Ajgaonkar, S. Tsuda, and M. Sharma, “Transparent ultra-long-haul DWDM networks with “broadcast-and-select” OADM/OXC architecture,” *J. Lightw. Technol.*, vol. 21, pp. 2661–2672, Nov. 2003.

[11] A. Boskovic, M. Sharma, N. Antoniades, and M. Lee, “Broadcast and select OADM nodes application and performance trade-offs,” in *Proc. Optical Fiber Communication Conf.* , 2002, pp. 158–159.

[12] D. T. Neilson, D. S. Greywall, S. Chandrasekhar, L. L. Buhl, H. Tang, L. Ko, N. R. Basavanhally, F. Pardo, D. A. Ramsey, J. D. Weld, Y. L. Low, J. Prybyla, R. Scotti, A. Gasparyan, M. Haueis, S. Arney, S. P. O'Neill, C.-S. Pai, D. H. Malkani, M. M. Meyers, N. Saluzzi, S. H. Oh, O. D. Lopez, G. R. Bogart, F. P. Klemens, M. Luo, J. Q. Liu, K. Teffeau, A. Ramirez, K. S. Werder, J. E. Griffith, C. Frye, M. V. Kunnavakkam, S. T. Stanton, J. A. Liddle, H. T. Soh, T-C. Lee, O. Nalamasu, and K. C. Nguyen, “High-dynamic range channelized MEMS equalizing filter,” in *Proc. Optical Fiber Communication Conf. Exhibit 2002*, 2002, pp. 586–588.

[13] D. T. Neilson, H. Tang, D. S. Greywall, N. R. Basavanhally, L. Ko, D. A. Ramsey, J. D. Weld, Y. L. Low, F. Pardo, D. O. Lopez, P. Busch, J. Prybyla, M. Haueis, C. S. Pai, R. Scotti, and R. Ryf, “Channel equalization and blocking filter utilizing micro electro mechanical mirrors,” *IEEE J. Select. Top. Quantum Electron.*, vol. 10, pp. 563–569, 2004.

[14] T. Zhou, D. O. López, M. E. Simon, F. Pardo, V. A. Aksyuk, and D. T. Neilson, “MEMS-based 14 GHz resolution dynamic optical filter,” *Inst. Elect. Electron. Lett.*, vol. 39, no. 24, pp. 1744–1745, 2003.

[15] D. M. Marom, D. T. Neilson, R. Ryf, and H. Shea, “Effect of mirror curvature in MEMS micro-mirror based wavelength-selective switches,” in *LEOS 2003 16th Ann. Meet.*, Tucson, AZ, Paper TuO4.

[16] X. Liu, L. F. Mollenauer, and X. Wei, “Impact of group-delay ripple in transmission systems including phase-modulated formats,” *IEEE Photon. Technol. Lett.*, vol. 16, pp. 305–307, Jan. 2004.

[17] F. Pardo, V. A. Aksyuk, S. Arney, H. Bair, N. R. Basavanhally, D. J. Bishop, G. R. Bogart, C. A. Bolle, J. E. Bower, D. Carr, H. B. Chan, R. Cirelli, E. Ferry, R. Frahm, A. Gasparyan, J. V. Gates, C. R. Giles, L. Gomez, S. Goyal, D. S. Greywall, M. Haueis, R. C. Kellera, J. Kim, F. P. Klemens, P. Kolodner, A. Kornblit, T. Kroupenkine, W. Lai, V. Lifton, J. Q. Liu, Y. Low, W. Mansfield, D. Marom, J. F. Miner, D. T. Neilson, M. Paczkowski, C.-S. Pai, A. Ramirez, D. Ramsey, S. Rogers, R. Ryf, R. Scotti, H. Shea, M. E. Simon, H. T. Soh, H. Tang, J. A. Taylor, K. Teffeau, J. Vuillemin, and J. Weld, “Optical MEMS devices for telecom systems,” in *SPIE's First Int. Symp. Microtechnologies for the New Millennium 2003: Smart Sensors, Actuators, and MEMS [5116–59]*, May 2003.

[18] D. Lopez, M. E. Simon, F. Pardo, V. Aksyuk, F. Klemens, R. Cirelli, D. T. Neilson, H. Shea, T. Sorsch, E. Ferry, O. Nalamasu, and P. L. Gammel, “Monolithic MEMS optical switch with amplified out-of-plane angular motion,” in *MOEMS 2002 Int. Conf. Optical MEMs*, Lugano, Switzerland, Aug. 2002, Paper ThB5.

[19] D. Lopez, F. Pardo, V. Aksyuk, M. E. Simon, H. R. Shea, D. M. Marom, D. T. Neilson, R. Cirelli, F. Klemensa, W. Mansfield, L. Fettera, E. Bower, J. Miner, and T. Sorsch, “MEMS mirror array for a wavelength selective 1 × K switch,” in *SPIE's First Int. Symp. Microtechnologies for the New Millennium 2003: Smart Sensors, Actuators, and MEMS [5116–59]*, May 2003.

[20] D. S. Greywall, P. Chien-Shing, O. Sang-Hyun, C. Chorng-Ping, D. M. Marom, P. A. Busch, R. A. Cirelli, J. A. Taylor, F. P. Klemens, T. W. Sorsch, J. E. Bower, W. Y.-C. Lai, and H. T. Soh, "Monolithic fringe-field-activated crystalline silicon tilting-mirror devices," *J. Microelectromech. Syst.*, vol. 12, no. 5, pp. 702–707, Oct. 2003.

[21] D. M. Marom and S. Oh, "Filter-shape dependence on attenuation mechanism in channelized dynamic spectral equalizers," in *15th Ann. Meet. Lasers and Electro-Optics Soc.*, vol. 2, Nov. 13–14, 2002, pp. 416–417.

[22] L. Möller, Y. Su, X. Liu, J. Leuthold, and C. Xie, "Ultrahigh-speed optical phase correlated data signals," *IEEE Photon. Technol. Lett.*, vol. 15, pp. 1597–1599, Nov. 2003.

[23] D. Penninckx and O. Audouin, "Optically preamplified systems: defining a new eye aperture," in *Optical Fiber Communication Conf. Exhibit 1998*, 1998, Paper WM36.

Roland Ryf (M'03) received the B.S. degree equivalent degree in electrical engineering from the Interstate University of Applied Sciences of Technology Buchs, Switzerland, in 1990 and the diploma and the Ph.D. degree in physics from the Swiss Federal Institute of Technology (ETH) Zürich, Switzerland, working on photorefractive self-focusing and spatial solitons, parallel optical processing based on holographic storage, and fast optical correlation, in 1995 and 2000, respectively.

Since May 2000, he has been working in the Photonic Subsystems and the Advanced Photonics Research Departments at Bell Laboratories, Lucent Technologies, Holmdel, NJ, where he is working on the optical design and prototyping of optical microelectromechanical systems (MEMs)-based devices. In particular large port count crossconnect switches, programmable spectral filters, dispersion compensators, and beam steering applications for free space optics communication. He has over 40 publications and 5 patents in the field of optical switching.

Yikai Su (M'01) received the B.S. degree from Hefei University of Technology, China, in 1991, the M.S. degree from Beijing University of Aeronautics and Astronautics, China, in 1994, and the Ph.D. degree from Northwestern University, Evanston, IL, in 2001.

He was with Crawford Hill, Bell Laboratories, Holmdel, NJ, for three years before he joined Shanghai Jiao Tong University, Shanghai, China, as a full professor in 2004. His research areas cover transparent optical networks, ultra high-speed transmission, and packet-switched networks. He has more than 60 publications in prestigious international journals and conferences, including eight invited conference papers. He holds one U.S. patent with three others pending.

Prof. Su serves as a Technical Committee Member of ICCCAS'04 and ICOCN'04, as well as a reviewer of the IEEE PHOTONICS TECHNOLOGY LETTERS, *Optics Letters*, *Optical and Laser Technology*, *Institution of Electrical Engineers Proc-OptoElectronics*, the *Journal of Optical Networking*, and the IEEE TRANSACTIONS ON CIRCUITS AND SYSTEMS II.

Lothar Möller (M'02) received the Dipl.-Phys. and Dipl.-Ing. degrees in physics and electrical engineering from RWTH Aachen, Germany, in 1992 and 1993, respectively, and the Ph.D. degree in communication techniques from ETH Zurich, Switzerland, in 1996.

In 1997, he joined Lucent Technologies Network Systems GmbH, Nuremberg, Germany. He then joined Bell Labs, Holmdel, NJ, in 1998. He has authored and coauthored several papers in the fields of signal equalization, polarization mode dispersion, and ultra high-speed data transmission.

S. Chandrasekhar (M'90–SM'00–F'01) received the B.Sc., M.Sc., and Ph.D. degrees in physics from the University of Bombay, Bombay, India, in 1973, 1975, and 1985, respectively.

He joined the Tata Institute of Fundamental Research, Bombay, India, as a Research Scholar in 1975 and then became a Research Associate in 1979. He had been engaged in research on Si–SiO_2 interface studies, complementary metal–oxide–semiconductor integrated circuits, ion implantation, charge-coupled devices, and laser recrystallization. In 1986, he joined AT&T Bell Laboratories (now called Lucent Technologies, Bell Laboratories), Crawford Hill Laboratory, Holmdel, NJ, as a Postdoctoral Member of Technical Staff. Since then, he has been working on III–V compound semiconductor devices for optoelectronic applications, primarily waveguides, photodetectors, heterojunction phototransistors, and heterojunction bipolar transitors (HBTs). He became a permanent Member of Technical Staff in May 1992. He has been engaged in high-speed optoelectronic integrated circuits (OEICs), integrating p-i-n photodetectors and laser diodes with HBTs, for long-wavelength optical communications. Since January 1999, he has been responsible for forward-looking research in wavelength-division-multiplexing (WDM) optical networking. He has set up an optical networking testbed for investigation of optical networks comprising add/drop multiplexers, optical cross connects, and wavelength-selective switching. His current interests include 40-Gb/s transport and networking, modulation formats, and electronic signal processing at the receiver. He is currently a Distinguished Member of Technical Staff. He holds 13 U.S. patents.

Dr. Chandrasekhar is a Member of the IEEE Lasers & Electro-Optics Society (LEOS). He has been Associate Editor of IEEE PHOTONICS TECHNOLOGY LETTERS since 1998. He has been member of the technical program committes of the International Electron Devices Meeting (IEDM), the Device Research Conference (DRC), and the Optical Fiber Communications (OFC) conferences. He was awarded the IEEE LEOS Engineering Achievement for 2000 jointly with two other awardees for his contribution to OEIC photoreceivers and the Optical Society of America (OSA) Engineering Excellence Award for 2004 for his contributions to OEICs and WDM systems research.

Xiang Liu (M'96) received the B.S. degree from Beijing Normal University, China, in 1989 and the M.S. degree from the Institute of Physics, Chinese Academy of Sciences, in 1994, both in physics. He received the Ph.D. degree in applied physics from Cornell University, Ithaca, NY, in 2000.

His doctoral work was on ultrafast optics and spatiotemporal solitons. He joined Bell Laboratories, Lucent Technologies, as a Member of Technical Staff in 2000. Since then, he has been primarily working on next-generation optical fiber communications technologies, including advanced modulation formats, mitigation of nonlinear penalties in high-speed transmissions, novel dispersion managements, forward-error-correction, and mitigation of polarization-mode dispersion, through analytical modeling, numerical simulation, and experiments. He has authored or coauthored approximately 60 archival journal papers and 30 conference papers. He has received several international patents.

David T. Neilson (M'96–SM'02) received the B.Sc. (Hons) degree in physics and the Ph.D. degree, also in physics, for work on optical nonlinearities in InGaAs quantum-well devices, both from Heriot-Watt University, U.K., in 1990 and 1993, respectively.

From 1993 to 1996, he was a Postdoctoral Researcher with Heriot-Watt University, where he worked on systems and devices for free-space optical interconnects. From 1996 to 1998, he was a Visiting Scientist with NEC Research Institute, Princeton, NJ, where he conducted research on optical interconnects for high performance computing. In 1998 he joined Bell Labs where he has worked on MEMS-based crossconnects, wavelength selective switches, equalizers, and dispersion compensators. He is currently a Technical Manager with responsibility for optoelectronic device growth and fabrication facility. He has more than 90 publications and 11 patents in the field of optical interconnects and switching.

Dr. Neilson is a Senior Member of the IEEE Lasers & Electro-Optics Society (LEOS) and a Member of the Optical Society of America (OSA).

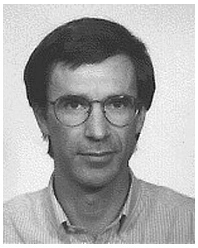

C. Randy Giles is a graduate of the University of Alberta and the University of Victoria.

He formerly worked at Nortel's research laboratories on their first gigabit optical transmission systems. Subsequently, In his 16-year career at Bell Laboratories, he pioneered the modeling and use of erbium-doped fiber amplifiers for lightwave systems, demonstrated the first optical add/drop multiplexers by means of Bragg-grating technology, and developed optical network applications of micromachines, including scalable optical cross connects and add/drop multiplexers. He is currently Director of the Advanced Photonics Research Department at Lucent Technologies, Holmdel, NJ. Research programs in his department include the study of new optical materials, the characterization and utilization of light in optical communications, and the development of optical networking technologies.

Dr. Giles is a Fellow of the Optical Society of America (OSA) and was awarded the 2001 Bell Laboratories Fellow.